CLM-R 34

CLM-R 34

United Kingdom Atomic Energy Authority

RESEARCH GROUP

Report

TRACING OF OBLIQUE RAYS IN PLASMA CYLINDERS

M. A. HEALD

Culham Laboratory,

Culham, Abingdon, Berkshire

1964

Available from H. M. Stationery Office

FOUR SHILLINGS NET

U.D.C.
533.951.7
533.93

UNCLASSIFIED
(Approved for Sale)

CLM - R 34

TRACING OF OBLIQUE RAYS IN PLASMA CYLINDERS

by

M. A. HEALD*

*U.S. National Science Foundation, Science Faculty Fellow, 1963 - 64.
Permanent address: Dept. of Physics, Swarthmore College, Swarthmore, Pa., U.S.A.

A B S T R A C T

The trajectory of an oblique ray in an axially symmetric inhomogeneous medium is formulated in the geometrical optics approximation. The attenuation due to electron-ion collisions and the angular deflection of a microwave ray traversing a cylindrical plasma column are evaluated, together with the statistical averages of these quantities over impact parameter and obliquity angle. The results of numerical computations for several simple electron-density profiles are shown graphically. These calculations are applicable to the theory of the microwave absorption and emissivity of a large, turbulent plasma[2,3].

U.K.A.E.A. Research Group,
Culham Laboratory,
Nr. Abingdon,
Berks.

February, 1964

(C/18 IMG)

CONTENTS

APPENDIX

1. INTRODUCTION

1. In reference (1) D.J.H. Wort considered the geometrical optics of microwave diagnostic beams incident normally on plasma cylinders of parabolic electron-density profile. That analysis then served as the basis for an elementary statistical treatment of the emissivity of a turbulent plasma[2]. A major limitation of that treatment was the assumption that the cylindrical turbulence elements were all parallel to each other, i.e., that the radiation transport was entirely two-dimensional. The present report provides the generalised geometrical optics analysis for obliquely incident rays and also, by numerical computation, considers profile models other than parabolic. This analysis is applied to the emissivity problem in reference (3).

2. SNELL'S LAW IN THREE DIMENSIONS

2. To handle the generalised problem it is necessary to develop Snell's law in three dimensions. However we restrict ourselves to axially symmetric cylinders with refractive index $\mu(r)$ a function of radius only and going to unity at $r \geqslant 1$ (we assume all space variables normalised to the cylinder radius). The co-ordinates of a point in the ray trajectory are (r, θ, z). At any point the angle between the tangent to the ray and the transverse $(r-\theta)$ plane is ω. The projection of the tangent on the transverse plane makes an angle φ with the radius vector. Thus the direction cosines of an element of the ray at any point are $(\cos\varphi\cos\omega, \sin\varphi\cos\omega, \sin\omega)$. A particular ray is specified by the impact parameter $b = \sin\varphi_0$ and the obliquity angle $\Omega = \omega_0$ at the point where the ray enters the cylinder. Note that the ray path may be broken into two symmetric halves about the point where $\underline{r}$ is a minimum $(\cos\varphi\cos\omega = 0)$, and that the parameters φ and ω return to the values $\varphi_0 = \sin^{-1}b$ and $\omega_0 = \Omega$ at the point where the ray leaves the cylinder.

3. We consider a boundary between two layers of a radially stratified medium, as represented by the heavy surface passing through the point O at co-ordinates (r, θ, z) in Fig.1. The ray passes through a cell of dimensions $(dr_1, d\theta_1, dz_1)$ and index μ to the point O, and thence through a cell of dimensions $(dr_2, d\theta_2, dz_2)$ and index $\mu+d\mu$. The ray direction is specified by (φ, ω) at the midpoint A of cell 1 and by $(\varphi+d\varphi, \omega+d\omega)$ at the midpoint B of cell 2. It is necessary to establish relations among the differentials, in terms of the angles φ and ω. If the length of the ray segment AO is denoted by L, then the direction cosines at point A yield the relations:

$$L \cos\varphi \cos\omega = \tfrac{1}{2}\, dr_1 - r(1 - \cos \tfrac{1}{2}\, d\theta_1) \ , \qquad \ldots (1)$$

$$L \sin\varphi \cos\omega = r \sin \tfrac{1}{2}\, d\theta_1 \ , \qquad \ldots (2)$$

$$L \sin\omega = \tfrac{1}{2}\, dz_1 \ . \qquad \ldots (3)$$

4. It is useful first to invoke the physical condition that the projection of the ray in the plane tangent to the interface at point O be undeviated. The angle t_1 between this projection of segment AO and the z direction is given by

$$\tan t_1 = \frac{(r - \tfrac{1}{2}\, dr_1)\sin \tfrac{1}{2}\, d\theta_1}{\tfrac{1}{2}\, dz_1} = \sin\varphi \cot\omega \left(1 - \tfrac{1}{2}\frac{dr_1}{r}\right) . \qquad \ldots (4)$$

The corresponding relation for cell 2 is

$$\tan t_2 = \sin(\varphi + d\varphi) \cot(\omega + d\omega) \left(1 + \tfrac{1}{2}\frac{dr_2}{r}\right) \qquad \ldots (5)$$

Demanding equality of the two expressions for $\tan t$, putting $\tfrac{1}{2}(dr_1 + dr_2) = dr$, and expanding to first order, one obtains the differential equation

$$\frac{dr}{r} + \cot\varphi\, d\varphi - \frac{d\omega}{\sin\omega \cos\omega} = 0 \ , \qquad \ldots (6)$$

which can be integrated immediately to yield

$$r \sin\varphi \cot\omega = \text{constant} = b \cot\Omega \ . \qquad \ldots (7)$$

5. We now wish to compute the angle of incidence of the ray segment AO with respect to the tangent plane at O. The square of the perpendicular distance p from point A to the radius vector through O is

$$\begin{aligned} p^2 &= [(r - \tfrac{1}{2}\, dr_1) \sin \tfrac{1}{2}\, d\theta_1]^2 + (\tfrac{1}{2}\, dz_1)^2 \ , \\ &= L^2 \sin^2\varphi \cos^2\omega \left(1 - \tfrac{1}{2}\frac{dr_1}{r}\right)^2 + L^2 \sin^2\omega \ , \qquad \ldots (8) \\ &= L^2\left[1 - \cos^2\varphi \cos^2\omega - \left(\frac{dr_1}{r} - \tfrac{1}{4}\frac{dr_1^2}{r^2}\right)\sin^2\varphi \cos^2\omega\right] , \end{aligned}$$

and thus the angle of incidence i is given to first order by the relation

$$\sin^2 i = \frac{p^2}{L^2} = 1 - \cos^2\varphi \cos^2\omega - \frac{dr_1}{r} \sin^2\varphi \cos^2\omega \ . \qquad \ldots (9)$$

A similar argument in cell 2 yields for the angle of refraction r ro first order

$$\begin{aligned} \sin^2 r &= 1 - \cos^2(\varphi + d\varphi) \cos^2(\omega + d\omega) + \frac{dr_2}{r} \sin^2\varphi \cos^2\omega \\ &= 1 - \cos^2\varphi \cos^2\omega + 2d\varphi \sin\varphi \cos\varphi \cos^2\omega \\ &\quad + 2d\omega \cos^2\varphi \sin\omega \cos\omega + \frac{dr_2}{r} \sin^2\varphi \cos^2\omega \ . \qquad \ldots (10) \end{aligned}$$

Now finally invoking Snell's law,

$$\mu \sin i = (\mu + d\mu) \sin r \ , \qquad \ldots (11)$$

and putting $\frac{1}{2}(dr_1 + dr_2) = dr$ and $d\mu/dr = \mu'$, we obtain the differential equation

$$\left(\frac{1}{r} + \frac{1 - \cos^2\varphi \cos^2\omega}{\sin^2\varphi \cos^2\omega} \frac{\mu'}{\mu} \right) dr + \cot\varphi \, d\varphi + \cot^2\varphi \tan\omega \, d\omega = 0 \ . \qquad \ldots (12)$$

Elimination of φ by means of (7) reduces (12) to

$$\frac{\mu'}{\mu} dr + \cot\omega \, d\omega = 0 \qquad \ldots (13)$$

which integrates immediately to

$$\mu \sin\omega = \text{constant} = \sin\Omega \ , \qquad \ldots (14)$$

permitting (7) to be rewritten as

$$\mu \, r \sin\varphi \cos\omega = \text{constant} = b \cos\Omega \ . \qquad \ldots (15)$$

Equations (14) and (15) represent two 'constants of motion' of the ray trajectory, the desired generalisation of Snell's law.

3. RAY PATH INTEGRALS

6. The direction cosines (ℓ, m, n) of the ray, in the (r, θ, z) directions respectively, can be expressed as:

$$m = \sin\varphi \cos\omega = \frac{b \cos\Omega}{\mu r} \qquad \ldots (16)$$

$$n = \sin\omega = \frac{\sin\Omega}{\mu} \qquad \ldots (17)$$

$$\ell = \cos\varphi \cos\omega = \pm (1 - m^2 - n^2)^{\frac{1}{2}} \qquad \ldots (18)$$

The ray penetrates to a minimum value of the radius r_{min} given by the condition $\ell = 0$, that is,

$$\mu^2(r_{min}) r_{min}^2 - r_{min}^2 \sin^2\Omega - b^2 \cos^2\Omega = 0 \ . \qquad \ldots (19)$$

Thus if $\mu(r)$ the initial conditions (b,Ω) are specified, r_{min} may be determined immediately without explicit solution of the ray path. However to obtain the angular deflection of the ray, and such quantities as the optical path and total attenuation, one must follow the full ray trajectory. The derivatives of the ray path are:

$$\frac{dz}{dr} = \frac{n}{\ell} = \frac{\tan\omega}{\cos\varphi} = \pm \frac{r \sin\Omega}{(\mu^2 r^2 - r^2 \sin^2\Omega - b^2 \cos^2\Omega)^{\frac{1}{2}}} \ , \qquad \ldots (20)$$

$$\frac{r d\theta}{dr} = \frac{m}{\ell} = \tan\varphi = \pm \frac{b \cos\Omega}{(\mu^2 r^2 - r^2 \sin^2\Omega - b^2 \cos^2\Omega)^{\frac{1}{2}}} \ . \qquad \ldots (21)$$

Note that the proper sign of the square-root must be taken, according to whether the ray

is proceeding toward smaller or larger radius. These equations may in principle be integrated to give $z(r)$ and $\theta(r)$ for the ray path. However even for the simplest inhomogeneity functions $\mu(r)$ and the special case $\Omega = 0$, analytic integration is difficult[1].

7. One may also obtain the arc-length s along the trajectory from the relation

$$\frac{ds}{dr} = \frac{1}{\ell} = \frac{1}{\cos\varphi\,\cos\omega} = \pm \frac{\mu r}{(\mu^2 r^2 - r^2\sin^2\Omega - b^2\cos^2\Omega)^{\frac{1}{2}}} \quad . \qquad \ldots (22)$$

The optical path is then

$$P = \int_{\text{path}} \mu\,ds = 2\int_{r_{min}}^{1} \frac{\mu^2 r\,dr}{(\mu^2 r^2 - r^2\sin^2\Omega - b^2\cos^2\Omega)^{\frac{1}{2}}} \quad , \qquad \ldots (23)$$

and Wort's attenuation parameter for isothermal electron-ion collisions[1] is *

$$Q = \int_{\text{path}} \frac{(1-\mu^2)^2}{4\mu}\,ds = 2\int_{r_{min}}^{1} \frac{\frac{1}{4}(1-\mu^2)^2 r\,dr}{(\mu^2 r^2 - r^2\sin^2\Omega - b^2\cos^2\Omega)^{\frac{1}{2}}} \quad . \qquad \ldots (24)$$

Again, these integrals are difficult to carry out analytically.

8. One is also interested in the deviation of the ray from its initial direction. For the special case of normal incidence (putting $\Omega = 0$), or if one considers only the deviation of the projection of the ray path in a transverse plane, the deviation angle is

$$\Psi_\perp = 2\cos^{-1} b - 2b\cos\Omega \int_{r_{min}}^{1} \frac{dr}{r(\mu^2 r^2 - r^2\sin^2\Omega - b^2\cos^2\Omega)^{\frac{1}{2}}} \quad . \qquad \ldots (25)$$

On the other hand the total deviation of the obliquely incident ray is

$$\Psi_{total} = \cos^{-1}(\cos\Psi_\perp \cos^2\Omega + \sin^2\Omega) \quad . \qquad \ldots (26)$$

Specular reflection occurs when the plasma is of high density so that the critical layer lies close to the surface or when Ω approaches $\pi/2$. One then has

$$\Psi_\perp \to \cos^{-1}(2b^2 - 1) = 2\cos^{-1} b \quad . \qquad \ldots (27)$$

---

* The fractional power loss of a wave is

$$\exp\left[-\frac{G\,n_c\,Z}{c(kT)^{\frac{3}{2}}}\,4\,r_o\,Q\right] ,$$

where r_o is the normalising scale of length, taken here to be the cylinder radius. The 'constant' G in fact varies slowly as $\log(T_e^{\frac{3}{2}}\,n_c^{-\frac{1}{2}})$ with the approximate value 3.10^{-5} $ev^{\frac{3}{2}}$-cm^3-sec^{-1} for common plasmas[4].

4. STATISTICAL AVERAGING

9. In the application to emissivity of a turbulent plasma[2] it is necessary to perform averages over the impact parameter $\underline{b}$, and perhaps also over the obliquity angle Ω[3]. Thus for the attenuation factor Q

$$\overline{Q}(\Omega) = \int_0^1 Q(\Omega,b)\ db \quad , \qquad \ldots (28)$$

$$\overline{\overline{Q}} = \int_0^{\pi/2} \overline{Q}(\Omega)\ \cos\Omega\ d\Omega \quad , \qquad \ldots (29)$$

the $\cos\Omega$ term in the latter integral being the usual solid-angle weighting factor. Although these integrals appear to be of fairly simple form, the difficulty of obtaining an analytic expression for $Q(\Omega,b)$ from equation (24) blocks further progress. Since the r_{min} limit of the $\underline{r}$-integration of (24) depends upon $\underline{b}$, it is unfortunately not possible to invert the order of integration, performing the simpler $\underline{b}$-integration (28) first.

10. The corresponding integrals for the mean-square deflection are

$$\overline{\Psi^2}(\Omega) = \int_0^1 \Psi^2(\Omega,b)\ db \quad , \qquad \ldots (30)$$

$$\overline{\overline{\Psi^2}} = \int_0^{\pi/2} \overline{\Psi^2}(\Omega)\ \cos\Omega\ d\Omega \ . \qquad \ldots (31)$$

For the specular-reflection limit ($n \gg n_c$ or $\Omega \to \pi/2$) we have from equation (27)

$$\overline{\Psi^2} \to \int_0^1 (2\cos^{-1}b)^2 db = 4(\pi - 2) = (122.5 \text{ degrees})^2 \ . \qquad \ldots (32)$$

5. THE PARABOLIC DISTRIBUTION

11. The most tractable electron-density profile for performing the ray-path integrals is the parabolic distribution

$$n/n_c = K(1 - r^2) \ , \qquad \ldots (33)$$

where K is the normalised electron density at the axis. Thus the refractive index is

$$\mu^2 = 1 - n/n_c = 1 - K(1 - r^2) \ . \qquad \ldots (34)$$

This case has been extensively studied in reference (1). We here recapitulate some of those results and add a few new ones. From equation (24) one obtains for normal incidence

$$Q(\Omega = 0) = \frac{3K^2 + 2K(1 + 2b^2) + 3}{32\ K^{1/2}} \tanh^{-1}\left[\frac{2K^{1/2}(1 - b^2)^{1/2}}{K + 1}\right] - \frac{3}{16}(K + 1)(1 - b^2)^{1/2} \ . \qquad \ldots (35)$$

The $\underline{b}$-integration can be carried out analytically for this case to obtain

$$\bar{Q}(\Omega = 0) = \frac{\pi}{48K}\left[(1 + K^3) \pm (1 - K^3) \right] ,$$

$$= \begin{cases} \frac{\pi}{24} K^2 & K \leqslant 1 \\ \frac{\pi}{24} \frac{1}{K} . & K \geqslant 1 \end{cases} \qquad \ldots (36)$$

From numerical computation it has been discovered that

$$\bar{Q}(\Omega) = \begin{cases} \frac{\pi}{24} \frac{K^2}{\cos \Omega} & K \leqslant \cos^2\Omega \leqslant 1 \\ \frac{\pi}{24} \frac{\cos^5\Omega}{K} . & K \geqslant \cos^2\Omega \end{cases} \qquad \ldots (37)$$

The fit of the numerical data to these formulae is so good that one presumes that they are exact, although this has not yet been proved. The condition

$$K = \cos^2\Omega , \qquad \ldots (38)$$

corresponds to the special case where the central ray $(b = 0)$ proceeds indefinitely along the cylinder axis, a non-physical artifact of geometrical optics. Assuming the formulae (37), one may then obtain

$$\bar{\bar{Q}} = \begin{cases} \frac{\pi}{24}\left[\frac{\pi}{2} K^2 + \left(\frac{5}{16K} - K^2 \right) \sin^{-1} K^{\frac{1}{2}} - \left(\frac{1 - K}{K} \right)^{\frac{1}{2}} \left(\frac{15 + 10K + 8K^2}{48} \right) \right] & K \leqslant 1 \quad \ldots (39) \\ \frac{5\pi^2}{768} \frac{1}{K} = \frac{5\pi}{32} \bar{Q}(\Omega = 0) . & K \geqslant 1 \quad \ldots (40) \end{cases}$$

The asymptotic expansions of (39) are

$$\bar{\bar{Q}} \approx \begin{cases} \frac{\pi^2}{48} K^2 - \frac{\pi}{28} K^{\frac{5}{2}} \left(1 + \frac{7K}{54} \right) & K \ll 1 \quad \ldots (41) \\ \frac{5\pi^2}{768} \frac{1}{K} - \frac{\pi (1 - K)^{\frac{3}{2}} (9 + K)}{120} . & 0 \leqslant (1 - K) \ll 1 \quad \ldots (42) \end{cases}$$

These expansions overlap at $K \approx \frac{2}{3}$, at which point they are in error by about + 3%. An empirical formula giving good fit ($\lesssim$ 3%) for $.1 < K < 1.0$ is

$$\bar{\bar{Q}} \approx 0.11\, K^2 (1.6 - K) . \qquad .1 \leqslant K \leqslant 1.0 \qquad \ldots (43)$$

Graphs of these quantities are included in the next section.

12. The transverse deflection from equation (25) is for normal incidence

$$\Psi(\Omega = 0) = \sin^{-1} \frac{2Kb(1 - b^2)^{\frac{1}{2}}}{[(1 - K)^2 + 4Kb^2]^{\frac{1}{2}}} . \qquad \ldots (44)$$

The maximum value of this deflection occurs where

$$b = \begin{cases} \left(\frac{1 - K}{2} \right)^{\frac{1}{2}} & K \leqslant 1 \\ 0 & K \geqslant 1 \end{cases} \qquad \ldots (45)$$

and is

$$[\Psi(\Omega=0)]_{max} = \begin{cases} \sin^{-1}K & K \leqslant 1 \\ \pi & K > 1 \end{cases} \quad \ldots (46)$$

Note the discontinuity in Ψ_{max} at $K = 1$. For the special case $K = 1$

$$\Psi(\Omega=0,\ K=1) = \cos^{-1}b \ , \quad \ldots (47)$$

and

$$\overline{\Psi^2}(\Omega=0,\ K=1) = \pi - 2 = (61.2 \text{ degrees})^2 \ . \quad \ldots (48)$$

Analytic expressions for $\overline{\Psi^2}$ and $\overline{\overline{\Psi^2}}$ have not been found. However equation (44) can be expanded for small K to give

$$\Psi(\Omega=0) \approx 2Kb(1-b^2)^{\frac{1}{2}}[1 + K(1-2b^2) + \ldots\ ]. \quad K \ll 1 \quad \ldots (49)$$

From this one obtains

$$\overline{\Psi^2}(\Omega=0) \approx \frac{8}{15} K^2\left(1 + \frac{2}{7} K + \frac{13}{63} K^2 + \ldots\right) \ . \quad K \ll 1 \quad \ldots (50)$$

An empirical formula valid ($\sim 3\%$) over the range $.2 < K < 1.0$ is

$$\overline{\Psi^2}(\Omega=0) \approx (\tanh^{-1} 0.77\ K)^2 \ . \quad .2 < K < 1.0 \quad \ldots (51)$$

Finally, an empirical formula for the obliquity-averaged quantity for small K is

$$\overline{\overline{\Psi^2}}_{total} \approx 1.6\ K^2\ (1 - .67K + .4K^2) \ . \quad K < .9 \quad \ldots (52)$$

6. NUMERICAL COMPUTATIONS

13. Because of the difficulty of evaluating Q, Ψ, and their averages analytically, especially for $\Omega \neq 0$ and for density profiles other than parabolic, two computer programs were written to perform the computation numerically. Program I followed individual ray trajectories in three dimensions (Fig.2) and then, by cycling through a large number of ray specifications (Ω and b) performed the integrations such as (28) - (31) in an elementary brute-force way. Program II was more efficient for performing the integrations but did not yield so much information about individual rays. The profiles were assumed in the form (compare equation 33)

$$n/n_c = K\ g(r) \ , \quad \ldots (53)$$

where the profile function $g(r)$ is such that

$$g(r = 0) = 1 \ ,$$
$$g(r \geqslant 1) = 0 \ . \quad \ldots (54)$$

The profiles considered and some of their properties are listed in Table 1. The 'line density' measures the amount of plasma contained in the cylinder per unit length. The

TABLE 1

profile	g(r)	line density $2\pi K \int_0^1 g\, r\, dr$	transverse density $2K \int_0^1 g\, dr$	W factor $\frac{\pi}{4} \int_0^1 g^2\, r\, dr$	approx. $\bar{Q}(K>0,\Omega=0)$ $\frac{\pi}{12} \frac{r_{eff}}{g'(r_{eff})}$ $[g(r_{eff}) = C/K]$
linear	$1 - r$	$\frac{\pi}{3} K$	K	$\frac{\pi}{48} = .065$	$\frac{\pi}{12} \frac{K-C}{K^2}$ $(C = \frac{3}{4})$
parabolic	$1 - r^2$	$\frac{\pi}{2} K$	$\frac{4}{3} K$	$\frac{\pi}{24} = .131$	$\frac{\pi}{24} \frac{C}{K}$ $(C = 1)$ (exact)
cubic	$1 - r^3$	$\frac{3\pi}{5} K$	$\frac{3}{2} K$	$\frac{9\pi}{160} = .177$	$\frac{\pi}{36} \frac{1}{K} \left(\frac{K}{K-C}\right)^{\frac{1}{3}}$ $(C = .879)$
*quartic	$1 - r^4$	$\frac{2\pi}{3} K$	$\frac{8}{5} K$	$\frac{\pi}{15} = .209$	
*uniform	$1\ (r < 1)$	πK	$2 K$	$\frac{\pi}{8} = .393$	
cosine	$\cos \frac{\pi}{2} r$	$\frac{4}{\pi} (\pi - 2) K$	$\frac{4}{\pi} K$	$\frac{\pi^2 - 4}{16\pi} = .117$	$\frac{1}{3\pi} \frac{\cos^{-1} C/K}{(K^2 - C^2)^{\frac{1}{2}}}$ $(C = .729)$
cos-squared	$\cos^2 \frac{\pi}{2} r$	$\frac{\pi^2 - 4}{2\pi} K$	K	$\frac{3\pi^2 - 16}{64\pi} = .068$	$\frac{1}{6\pi} \frac{\cos^{-1}(C/K)^{\frac{1}{2}}}{(K-C)^{\frac{1}{2}}}$ $(C = .147)$
*Bessel	$J_0(2.405\ r)$	$\frac{2\pi\ J_1(2.405)}{2.405} K = 1.36 K$	$\frac{4K}{2.405}(J_1+J_3+J_5+\ldots)_{2.405} = 1.22 K$	$\frac{\pi}{8} J_1^2(2.405) = .106$	

* Numerical computations not made; case listed for reference only.

'transverse density' represents the quantity measured by a microwave interferometer beam directed across a diameter. A comparison of these characteristics of the various profiles is given in Fig.3.

14. Figures 4 - 17 show results of these calculations, as follows:

Fig. 4	$Q(\Omega=0, b)$ for parabolic profile, i.e. equation (35)
Fig. 5	$\bar{Q}(\Omega=0)$
Figs.6-10	$\bar{Q}(\Omega)$ for various profiles
Fig.11	$\bar{\bar{Q}}(K)$
Fig.12	$\bar{\bar{Q}}$(line density)
Fig.13	$\bar{\bar{Q}}/\bar{Q}(\Omega=0)$
Fig.14	$\Psi(\Omega=0, b)$ for parabolic profile, equation (44)
Fig.15	$\overline{\Psi^2}(\Omega=0)$
Fig.16	$\overline{\Psi^2}_{total}(\Omega)$ for parabolic profile
Fig.17	$\bar{\bar{\Psi}}^2_{total}(K)$

15. It may be seen in Figs.6-10 that the $\bar{Q}(K,\Omega)$ curves divide into the portion in the range $K < \cos^2\Omega < 1$, which rises with increasing Ω, and the portion in the range $\cos^2\Omega < K$, which falls with increasing Ω. The maximum of $\bar{Q}$ is reached at the axial-ray condition (38), $\cos^2\Omega = K$. For all five cases tested it is found that the <u>former</u> region is precisely fitted by a formula of the form

$$\bar{Q} = \frac{K^2}{\cos\Omega} \cdot \frac{\pi}{4} \int_0^1 g^2(r)\, r\, dr \,. \qquad \ldots (55)$$

That is to say, it appears that in the range $K < \cos^2\Omega < 1$

$$\frac{\bar{Q}\cos\Omega}{K^2} \equiv \int_{b=0}^{1} \int_{r=r_{min}(b)}^{1} \frac{\tfrac{1}{2} g^2(r)\, r\, dr\, db}{\left[r^2 \left(1 - \frac{Kg(r)}{\cos^2\Omega}\right) - b^2\right]^{\frac{1}{2}}}$$

$$= \frac{\pi}{4} \int_{r=0}^{1} g^2(r)\, r\, dr \equiv W \,, \qquad \ldots (56)$$

although this equality has not yet been proved analytically. The W-constants are included in Table 1 and Fig.3.

16. No such general formula for the <u>second</u> range $\cos^2\Omega < K$ has been found, except for the parabolic case already mentioned in equation (37). However, a semi-quantitative argument for $K > 1$ suggests that $\bar{Q}(\Omega=0)$ should be proportional to the product of $Q(b=0)$ and an effective 'cross-section' radius. In turn $Q(b=0)$ may be estimated from the

reciprocal density gradient evaluated at the radius r_{crit} corresponding to critical density[1] and the 'cross-section' likewise taken as r_{crit}. Then

$$\bar{Q}(\Omega=0) \approx A \frac{r_{crit}}{K\, g'(r_{crit})} \qquad \ldots (57)$$

where $g(r_{crit}) = 1/K$ and $g'(r) \equiv dg/dr$. The proportionality constant A may be evaluated from the known result (36) for the parabolic profile, i.e. $A = \pi/12$. While this procedure is found to be reasonably satisfactory for $K \gg 1$, a further refinement is necessary for $K > 1$. Instead of evaluating the gradient and 'cross-section' at the critical radius r_{crit}, one can define an effective radius r_{eff} such that

$$g(r_{eff}) = C/K \qquad \ldots (58)$$

where C is chosen for each profile so as to make formula (57) fit at $K = 1$. This modification does not alter the asymptotic values for $K \gg 1$. The resulting forms of this approximation are given in Table 1. The agreement is good for all $K > 1$ points computed except in the case of the cosine-squared profile, which is also unique in that the asymptotic $\bar{Q}$ for $K \gg 1$ is proportional to $K^{-\frac{1}{2}}$ rather than K^{-1}. No systematic representation of the Ω-dependence of $\bar{Q}$ for $K > \cos^2\Omega$ has been found, except as noted in the parabolic case (37).

17. The variation of $\bar{\bar{Q}}$ with K and profile function is probably best seen by considering the ratio $\bar{\bar{Q}}/\bar{Q}(\Omega=0)$, Fig.13. For the parabolic case this ratio has the limits $\pi/2$ $(K \ll 1)$ and $5\pi/32 = 0.49$ $(K \gtrsim 1)$. The empirical formula (43) may be adapted to give for this ratio the value $.84(1.6 - K)$ in the range $.1 < K < 1$. All profile cases computed have $\bar{\bar{Q}}/\bar{Q}(0) \approx \frac{1}{2}$ for $K \gg 1$. When the different profile cases are compared for equal line densities (see Table 1) rather than equal central densities (K), the $\bar{\bar{Q}}/\bar{Q}(0)$ ratios remain only weakly dependent on profile. Likewise the $\bar{\bar{Q}}$ curves, when so compared (Fig.12), differ significantly only near their peaks, except for the rather anomalous cosine-squared profile.

18. The averaged angular quantities $\overline{\Psi^2}$ and $\overline{\overline{\Psi^2}}$, Figs.15 - 17, show obvious systematic trends. However no very useful approximate formulae have been found, except as already noted for the parabolic case, equations (50) - (52). The dependence of $(\overline{\Psi^2})^{\frac{1}{2}}$ and $(\overline{\overline{\Psi^2}})^{\frac{1}{2}}$ on profile for small K (i.e. small-angle scattering) is roughly in the ratio of the 'transverse density' factors of Table 1. When the curves are compared for equal line density, the different profile cases computed spread by only about ±20% in $\overline{\Psi^2}$ and ± 12% in $\overline{\overline{\Psi^2}}$.

7. CONCLUSIONS

19. The task of this report has been to set down, for future reference in connection with plasma turbulence problems, a large number of computational results for oblique rays traversing plasma cylinders of various electron-density profiles. The calculations are based entirely upon geometrical optics, assume an isothermal plasma, and also neglect effects due to the presence of a magnetic field. Thus due caution is required in applying the results to microwaves in laboratory plasmas. By resorting to numerical computation, a number of results are obtained which are not available analytically. In general, no strong dependence on profile model is found, although there are some systematic differences between the sharply bounded profiles (e.g. parabolic) and the more diffusely bounded case (cosine-squared). The application of these results to the microwave emissivity of a turbulent plasma is given in reference (3).

8. REFERENCES

1. WORT, D.J.H. Refraction of microwaves by a plasma cylinder. CLM-R 27. H.M.S.O., 1963.

2. WORT, D.J.H. The microwave emissivity of a turbulent plasma. J. Nuclear Energy, Part C, (In the press).

3. WORT, D.J.H. The microwave emissivity of a turbulent plasma, with random orientation of the turbulence elements, CLM-R 35. H.M.S.O., 1964.

4. HEALD, M.A. and WHARTON, C.B. Plasma Diagnostics with Microwaves, John Wiley and Sons, New York, 1964. Section 2-5.

APPENDIX

COMPUTER PROGRAM I

20. Rather than evaluating the integrals of equations (24) and (25) as such, the computer took a three-dimensional step along the ray in the direction prescribed by the direction cosines, and then recomputed the direction cosines at the new point from equations (16) - (18). This procedure was refined somewhat by carrying a running memory of the direction cosines at the previous point so that the step in r, for instance, was in fact computed as

$$\Delta r = \tfrac{1}{2}(3\ell - \ell')\Delta s \ , \qquad \ldots (59)$$

where ℓ and ℓ' are the current and previous values, respectively, of the radial direction cosine and Δs is the prescribed step along the arc of the trajectory. The computed increment may be seen to represent the second-order Taylor expansion

$$r(s+\Delta s) = r(s) + \left(\frac{dr}{ds}\right)_s \Delta s + \tfrac{1}{2}\left(\frac{d^2 r}{ds^2}\right)_s \Delta s^2 \qquad \ldots (60)$$

since $dr/ds = \ell$ and $d^2r/ds^2 = d\ell/ds \approx (\ell - \ell')/\Delta s$. The ray was followed in three dimensions in this manner from the entrance co-ordinates ($r_o = 1$, $\theta_o = \sin^{-1} b$, $z_o = -(1-b^2)^{\frac{1}{2}}\tan\Omega$) until the condition $\ell = 0$ was reached, signifying the mid-point of the ray trajectory at $r = r_{min}$. At each step the Q integrand $(1-\mu^2)^2/4\mu$ was evaluated and summed to provide the Q attenuation integral by the elementary trapezoidal rule. From the change in θ along the half-trajectory the transverse deflection was obtained as

$$\Psi_\perp = \pi - 2\,\theta(r = r_{min}) \ . \qquad \ldots (61)$$

The total deflection of equation (26) was not calculated in this program. The program also computed the optical path P of equation (23) and a quantity

$$\Delta z = 2\ z(r = r_{min}) \qquad \ldots (62)$$

measuring the offset of the ray in the z direction. However no use has been made of these two quantities so far. The Ω-integrals were performed both with and without the $\cos\Omega$ solid-angle weighting of equation (29).

21. A single data card called for computations to be made for a grid of values of K (the normalised electron density n/n_c at $r=0$), Ω (the obliquity angle), and $\underline{b}$ (the impact parameter). In addition to tracing the ray trajectory for each K-Ω-b condition, the computer evaluated $\bar{Q}$ and $\overline{\Psi_\perp^2}$ by trapezoidal integration over b, and finally $\bar{\bar{Q}}$ and $\overline{\overline{\Psi_\perp^2}}$ by trapezoidal integration over Ω, according to equations (28) - (31). The step length and integration interval were controlled by the data card in such a way that print-out

could be obtained at any desired multiple of the basic step or interval. Thus for instance one could obtain detailed print-out of the co-ordinates of a particular ray trajectory for one K-Ω-b condition or, alternatively, one could obtain the b and Ω integrations with minimum print-out of ray co-ordinates.

22. The special case of $K \geqslant 1$, $b = 0$ could not be handled by the type of ray tracing used; moreover for b non-zero but small the computer would have trouble negotiating the sharp curvature near the ray mid-point. To handle this problem the computer skipped the rays it could not cope with and then evaluated the b-integral by means of a linear extrapolation from the first two rays (of increasing b) that were computable. Some trouble with this procedure was experienced since the first computable ray was often traced with poor precision, and the resulting errors were then magnified by the extrapolation. The extrapolation formula used was, for k points omitted from an n-point trapezoidal integration: in place of

$$\bar{Q} = \left[\tfrac{1}{2} Q_1 + \sum_{j=2}^{n-1} Q_j + \tfrac{1}{2} Q_n \right] (n-1)^{-1}$$

substitute

$$\bar{Q} = \left[\tfrac{1}{2} (k+1)^2 Q_{k+1} - \tfrac{1}{2} (k^2-2) Q_{k+2} + \sum_{j=k+3}^{n-1} Q_j + \tfrac{1}{2} Q_n \right] (n-1)^{-1} . \quad \ldots (63)$$

In the initial trials of the program, convergence tests were made to determine reasonable choices of ray steplength to give better than ½% accuracy in the $\bar{Q}$ computations. In the case of the parabolic density profile the computer calculated r_{min} independently from equation (19) as a check, and also certain results for $\Omega = 0$ could be checked with known values[1].

COMPUTER PROGRAM II

23. This program evaluated directly the integrals of (24) - (25) by four-point Gaussian integration over initially large increments in r, which then progressively decreased in size as the integrand blew up (i.e. as r approached r_{min}). The averaging over impact parameter b, equations (28) and (30), was done by the six-point Gaussian prescription. The averaging over obliquity angle Ω, equations (29) and (31), was three-point Gaussian for the range $K < \cos^2\Omega$, if $K < 1$, and four-point Gaussian for the remaining range or for the entire range when $K > 1$. Thus minimum error accrued from the cusp-like behaviour of $\bar{Q}(\Omega)$ near $\Omega = \cos^{-1} K^{\frac{1}{2}}$ when $K < 1$. The single-bar (b-averaged) quantities were also obtained for $\Omega = 0$. Note that since the Gaussian integration over b never calls for $b = 0$, no trouble is experienced from rays which run away down the axis. However the values of $\bar{Q}(\Omega = 0)$ for $K = 0$ were found to be low by a few percent, presumably because the six-point Gaussian integration over b failed to cope accurately with the integrable infinity in Q at $b = 0$. Otherwise the accuracy in the $\bar{Q}$ calculations was estimated at about ½% and in $\bar{\bar{Q}}$, some 1 to 2%. Both $\Psi_\perp$ and Ψ_{total} were found for each (Ω, b) condition, but only Ψ^2_{total} was carried through the b and Ω averaging. The five profile functions of Table 1 were built into the program, the data card calling for the desired profile. Other profile functions could easily be substituted by re-compiling a subroutine.

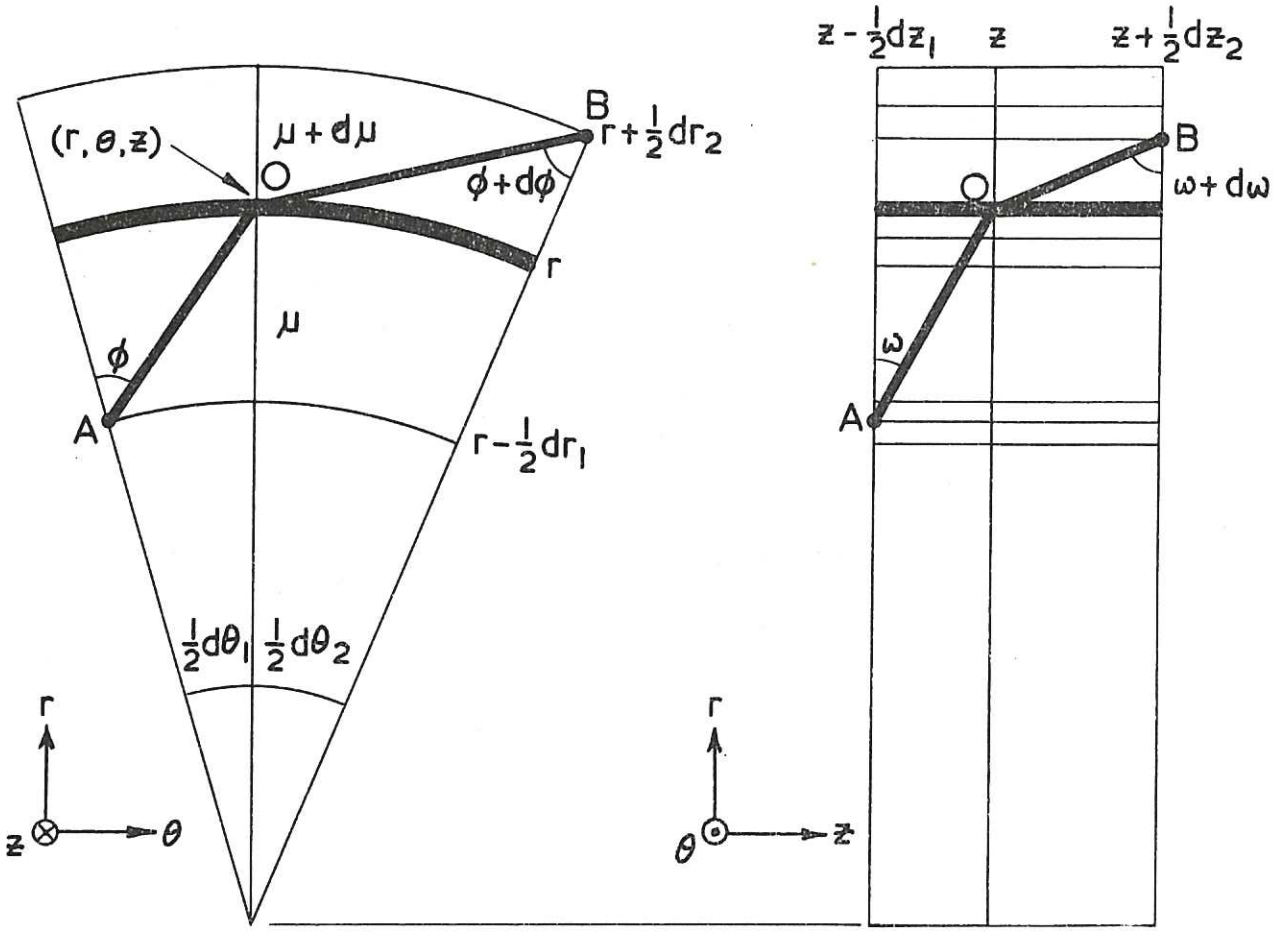

CLM-R34 Fig. 1

Geometry of a ray refracted at an interface in an axially symmetric inhomogeneous medium. If the point O is taken as in the plane of the drawing, then neither point A nor B lies in that plane. The angles ϕ, $\phi+d\phi$ measure the projection of the ray in the transverse plane and thus are properly shown in the left-hand drawing. The angles ω, $\omega+d\omega$ measure the actual oblique ray with respect to the transverse plane and are only schematically shown in the right-hand drawing.

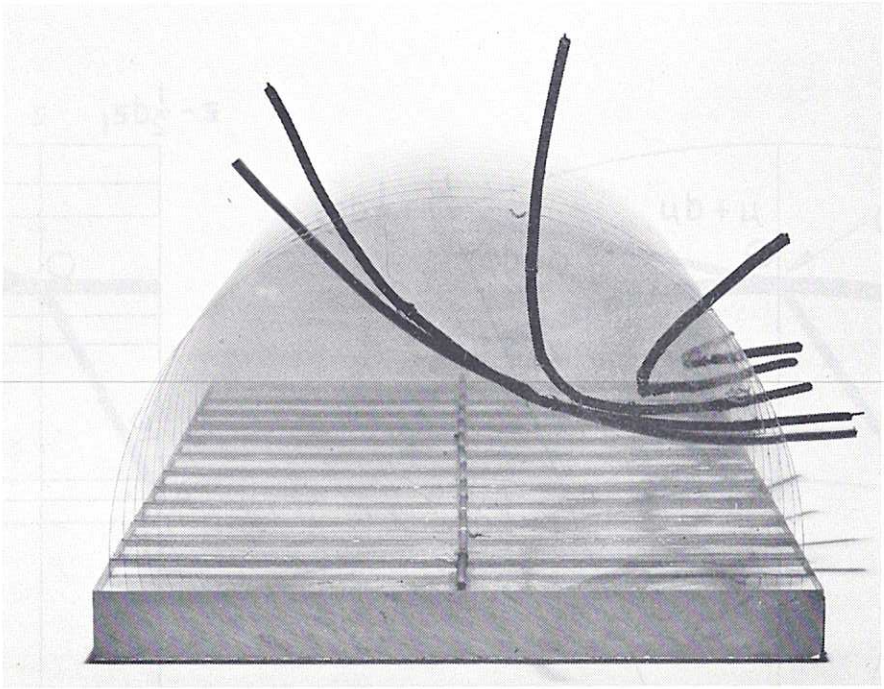

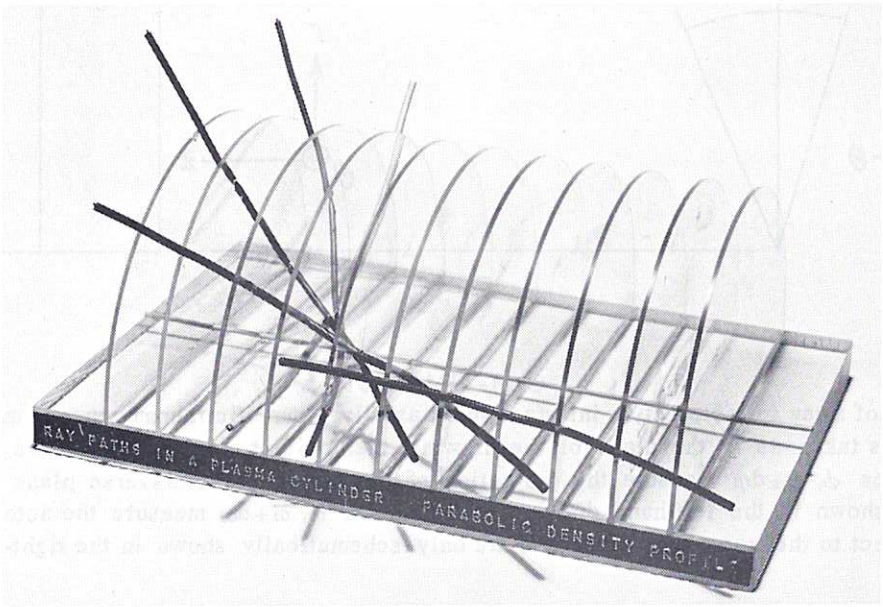

CLM-R 34 Fig. 2

Photographs of a model showing oblique rays for the parabolic density profile;
K = 0.8; b = 0.2; Ω = 0, 15, 30, 45, 60 degrees.

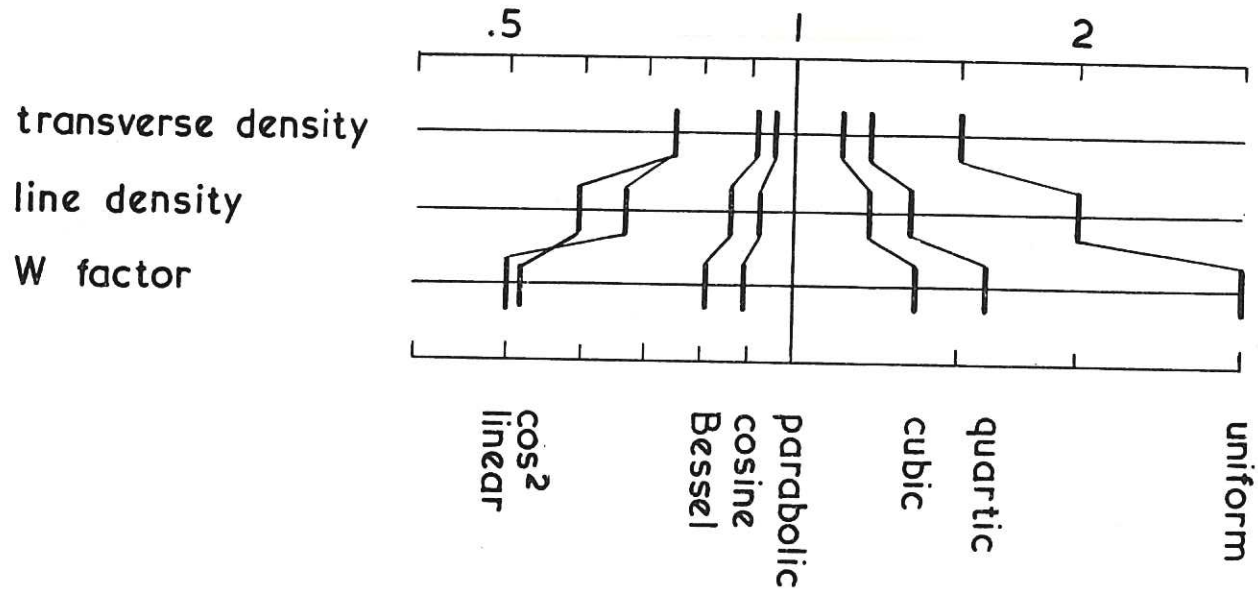

CLM-R 34 Fig. 3
Comparison of magnitudes of the parameters of Table 1, normalised to the parabolic profile case.

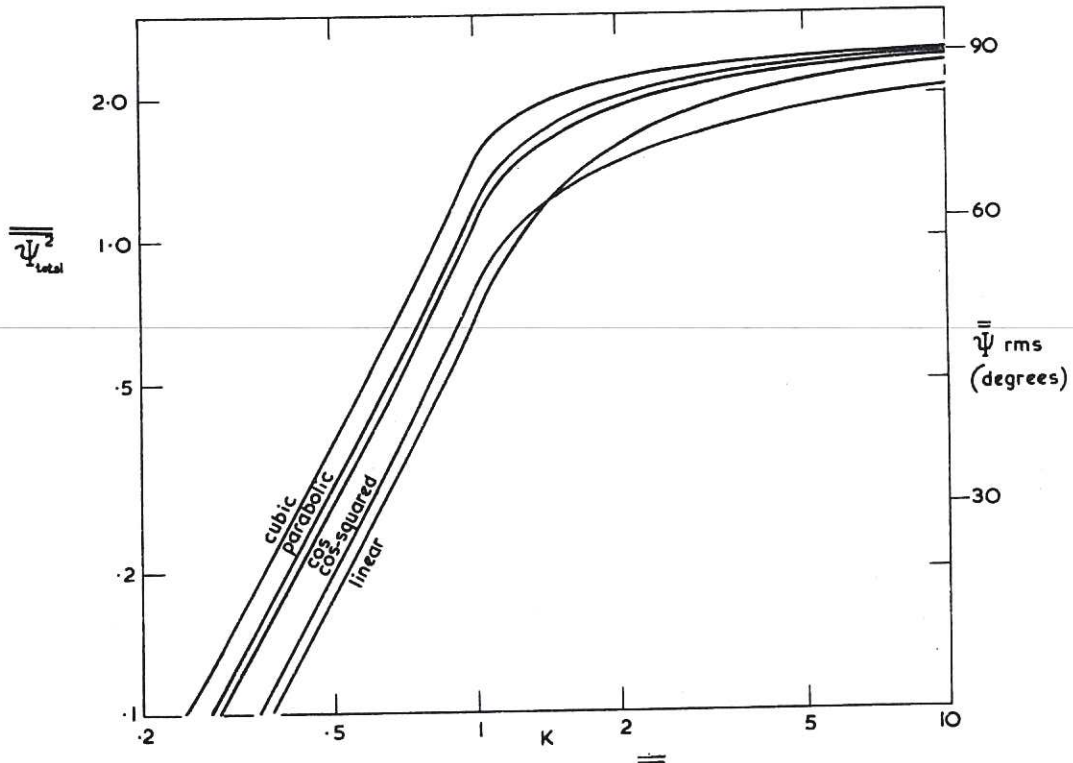

CLM-R34 Fig. 17 $\overline{\overline{\Psi^2}}_{total}$ vs K.

Available from
HER MAJESTY'S STATIONERY OFFICE
York House, Kingsway, London W.C. 2
423 Oxford Street, London W. 1
13a Castle Street, Edinburgh 2
109 St. Mary Street, Cardiff
39 King Street, Manchester 2
50 Fairfax Street, Bristol 1
35 Smallbrook, Ringway, Birmingham 5
80 Chichester Street, Belfast
or through any bookseller.

Printed in England

S.O. Code No. 91-3-15-36